Green Chemistry

CRITICAL REVIEW

View Article Online
View Journal | View Issue

Cite this: *Green Chem.*, 2016, **18**, 5736

Sustainable hybrid photocatalysts: titania immobilized on carbon materials derived from renewable and biodegradable resources

Juan Carlos Colmenares,*[a] Rajender S. Varma[b] and Paweł Lisowski*[a]

This review comprises the preparation, properties and heterogeneous photocatalytic applications of TiO_2 immobilized on carbon materials derived from earth-abundant, renewable and biodegradable agricultural residues and sea food waste resources. The overview provides key scientific insights into widely used TiO_2 supported on carbonaceous materials emanating from biopolymeric materials such as lignin, cellulose, cellulose acetate, bacterial cellulose, bamboo, wood, starch, chitosan and agricultural residues (biochar, charcoal, activated carbon and their magnetic forms, coal fly ash) or seafood wastes namely eggshell, clamshell and fish scales; materials that serve as a support/template for TiO_2. Heightened awareness and future inspirational developments for the valorisation of various forms of carbonaceous functional materials is the main objective. This appraisal abridges various strategies available to upgrade renewable carbon-based feedstock *via* the generation of sustainable TiO_2/carbon functional materials and provides remarks on their future prospects. Hopefully, this will stimulate the development of efficient and novel composite photocatalysts and engender the necessary knowledge base for further advancements in greener photocatalytic technologies.

Received 4th September 2016,
Accepted 20th September 2016

DOI: 10.1039/c6gc02477g

www.rsc.org/greenchem

[a]*Institute of Physical Chemistry, Polish Academy of Sciences Kasprzaka 44/52, 01-224 Warsaw, Poland. E-mail: jcarloscolmenares@ichf.edu.pl, plisowski@ichf.edu.pl; http://photo-catalysis.org*
[b]*Sustainable Technology Division, National Risk Management Research Laboratory, US Environmental Protection Agency, 26 West Martin Luther King Drive, MS 443, Cincinnati, Ohio, 45268, USA*

1. Introduction

The use of relatively non-toxic and earth-abundant local materials in chemical conversion is a prerequisite for the development of any sustainable process. Titanium dioxide

Juan Carlos Colmenares

Prof. Dr Juan Carlos Colmenares is graduated from Warsaw University of Technology in 1995 and obtained his MSc (1997) and PhD (2004) from the same University, and the scientific degree of habilitation (DSc 2015) from the Polish Academy of Sciences. His interests include materials science, nanotechnology, heterogeneous catalysis, biomass/CO_2 valorisation, solar chemicals, sonochemistry, photocatalysis and water/air purification. After obtaining his PhD, he conducted postdoctoral work at the University of Cordoba, Spain (2005–2006) in Prof. Marinas's group and at the University of Southern California, Los Angeles (USA) (2006–2009) in Prof. G. A. Olah's group.

Rajender S. Varma

Prof. Dr Rajender S. Varma (PhD, Delhi University 1976) was born in India. After postdoctoral research at Robert Robinson Laboratories, Liverpool, UK, he was a faculty member at Baylor College of Medicine and Sam Houston State University before joining the US Environmental Protection Agency in 1999. He has over 40 years of experience in the management of multidisciplinary programs in areas ranging from environmentally benign alternatives for synthesis using mechanochemical, microwave- and ultrasound irradiation, to technologies for remediation of contaminated sites. Lately, he works on greener assembly of nanomaterials and the application of magnetically retrievable nanocatalysts.

(TiO_2) is one of the most commonly used photocatalysts and carbon can be accessed from a wide variety of waste resources. Carbon-based materials have been utilized in environmental remediation and now making inroads into an emerging and conceptually new area of photocatalytic materials; their unique features need to be exploited for larger scale industrial use. While tremendous progress has been made in the syntheses of porous carbon-based materials with varying structure-types, challenging opportunities remain for the functionalization of these materials in terms of the optimization of their properties for specific applications namely separation science, filtration devices, photocatalyst supports and energy storage.[1–3] When compared to conventional resources, carbon materials possess outstanding properties such as hydrophobic surfaces, high surface area, large pore volume, chemical inertness, good thermal and mechanical stability, easy handling and low cost of manufacture, that will enable their enhanced use in energy-conversion and storage.[1–4] The synergistic effects of TiO_2 with carbon materials bearing enhanced multi-functionalities for use in heterogeneous photocatalysis, energy-storage, and solar cell applications, renders TiO_2 immobilized on porous carbon as a valuable material. In the area of environmental remediation, carbon materials offer a great potential for the efficient removal of pollutants in water and air,[5,6] as has been demonstrated by emerging heterogeneous photocatalysis as an alternative economical and benign technology for the purification of water and air.[7,8] From a practical point of view, alternative photocatalytic materials that can match the TiO_2 profile, namely versatility, inexpensiveness and abundance, and a non-toxic nature are hard to find. However, TiO_2 still has some shortcomings which prevent its widespread usage. First, the large band gap energy of TiO_2 (3.2 eV) limits its use exclusively to the ultraviolet region of the solar spectrum which accounts for only a very small fraction of the solar energy (about 3–5%).[9–13] Second is the need to support nanostructured titania for better filtration and material recovery. Although a significant amount of research has been conducted on TiO_2 photocatalysis at the laboratory scale its application on an industrial scale is limited, which needs to be addressed. To overcome the severe drawbacks of the most stable photocatalyst, TiO_2, namely its low efficiency, narrow light-response range and material recycling, many strategies have been developed *via* modification to acquire multifunctional materials that increase its photocatalytic activity for organic pollutant treatment;[14,15] comprehensive articles have documented these advancements in the field of TiO_2-based photocatalysts[3–9,16,17] and especially the use of carbon as a support for TiO_2.[18–22] Petroleum-derived polymers, when used as a support for TiO_2 (*e.g.* high-density polyethylene (HDPE),[23] polyaniline (PANI),[24] resorcinol-formaldehyde (RF)[25]), have drawbacks such as non-renewability, higher costs, and additional contribution to pollution.[26] Faced with such a dilemma, more and more attention has been paid to the development and application of natural materials as a support for TiO_2. In the context of green chemistry, natural renewable materials such as lignocelluloses and raw biomass are especially attractive for their unique physicochemical properties such as good electrical conductivity, higher surface area and excellent chemical stability.[27–30] We expect that such a comprehensive and critical review will provide key scientific insights into TiO_2/carbon materials derived from renewable and biodegradable resources emanating from biopolymeric materials such as lignin, cellulose, cellulose acetate, bacterial cellulose, bamboo, wood, starch, chitosan and agricultural residues (biochar, charcoal, activated carbon and their magnetic forms, coal fly ash) or seafood wastes (namely eggshell, clamshell and fish scales); materials that serve as a support/template for TiO_2. A keen awareness of future inspirational developments for the valorisation of various forms of carbonaceous functional materials is another objective. This review abridges different approaches or/and strategies which have been reported so far to upgrade renewable carbon-based feedstocks *via* the preparation of sustainable TiO_2/carbon functional materials and provides comments on their future prospects that will help stimulate the development of efficient and novel composite photocatalysts; the attained knowledge-base will boost advancements in greener photocatalytic technologies.

Paweł Lisowski

Paweł Lisowski is currently a PhD candidate at the Institute of Physical Chemistry of the Polish Academy of Sciences in Poland. He raduated from Radom University of Technology and obtained his MSc (2007) in Chemical Technology with specialization in protection of the environment and post-graduate studies in Analytical Chemistry in Industry and Environmental Protection at AGH University of Science and Technology located in Krakow, Faculty of Materials Science and Ceramics. His research currently covers various aspects of rational design and synthesis of new inorganic–organic hybrid materials from renewable materials as a carbon support with photocatalytic properties using unconventional methodologies.

2. Emerging role of carbonaceous materials in semiconductor photocatalysis

The semiconductor photocatalyst, TiO_2, is an important material that underpins the development of critical renewable energy and environmental technologies such as photocatalytic water/air purification, hydrogen production from water splitting, and high-efficiency/low-cost solar cells.[31] In photocatalysis, the electron/hole pairs are the photo-excited charge car-

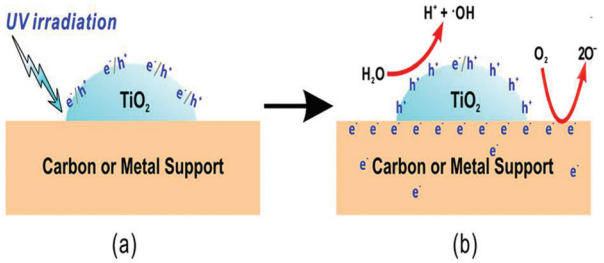

Fig. 1 Schematic illustrations of the proposed synergetic photocatalytic effect of the TiO_2/carbon support. Reproduced with permission from ref. 33.

riers on the conduction and valence bands, respectively. The free holes have strong oxidation power, while the oxygen radicals are secondary products of the electron reduction process;[32] a simplified mechanism for the synergetic photocatalytic effect of TiO_2/carbon support is presented in Fig. 1. TiO_2 is activated directly by UV light irradiation of photon energy higher than the band gap energy of titania, forming e^-/h^+ pairs (Fig. 1a). More importantly, carbon plays the central role of an electron reservoir to conduct away the electrons from the e^-/h^+ pairs on/in TiO_2, thus leading to the increased efficiency of charge separation in TiO_2; the activation of TiO_2, and in the meantime the activation of an electron-conductive phase (such as carbon) which activates O_2 to O^- ions, takes place (Fig. 1b).[33]

3. TiO_2/carbon materials derived from lignocellulosic materials

Carbon materials derived from biopolymers have made considerable progress in recent years, especially in the development of molecular sieves, as photocatalyst supports and adsorbents for the storage of natural gas.[26,34,35] Compared to the thermal method, photocatalytic polymerization is initiated with light and is terminated upon switching off the light. Furthermore, the molecular weight and density of the polymer can be varied through the selection of monomer and irradiation conditions. Carbonization of the carefully designed polymer provides opportunities in controlling the pore size, pore volume and bulk density of the ensuing carbon, which are important characteristics in the aforementioned applications.[26,34,35] The composition of lignocellulose biomass is highly dependent on its source (Fig. 2). There is a significant variation of the lignin and (hemi)cellulose components of the lignocellulose component on whether it is derived from hardwood, softwood, or grasses, extracts, or inorganic related materials.[36–38] Starch (as well as sugars), triglycerides and lignocellulose are the typical classes of feedstocks derived from biomass and are used for the production of renewable biofuels and chemicals. Lignin, a three-dimensional network macromolecule, is electronegative and has a strong affinity for the positively charged metal ions; lignin with phenolic

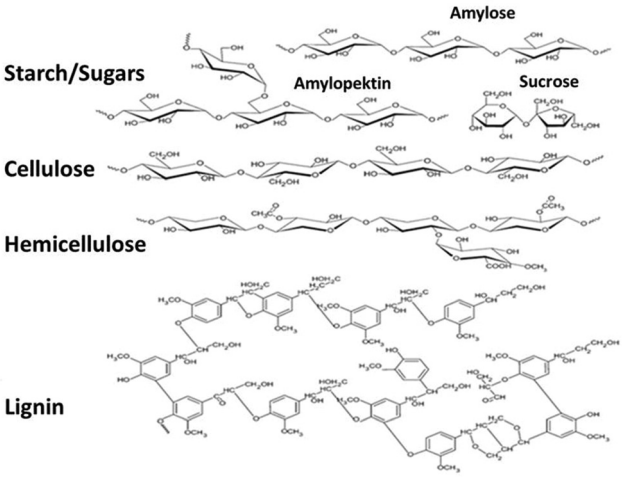

Fig. 2 Overview of the prominent fractions of the biomass feedstock.

hydroxyl-, alcoholic hydroxyl-, and carboxylic groups can react chemically with other polymers to form hybrid composites.[39] On the other hand, cellulose, an organic polysaccharide comprising a linear chain of several hundreds to many thousands of β(1→4) links *via* D-glucose units, is mainly used to produce paper and paperboard. It has multiple hydroxyl groups on one long chain to form hydrogen bonds with other oxygen atoms on the neighboring chain.[40]

3.1 TiO_2/lignin

Native unmodified lignin has been used as a template for the formation of mesoporous TiO_2 nanoparticles *via* a hydrolysis precipitation method exploiting the electronegativity and the network skeleton of lignin (see Fig. 3);[41] as-synthesized composite had a BET surface area of 165.8 $m^2\ g^{-1}$ and a pore volume of 0.312 $cm^3\ g^{-1}$. In view of the interactions between hydroxyl groups of lignin and the surface hydroxyl groups of the TiO_2 precursor, the calcined TiO_2 particles have a finer crystallite size, a mesoporous structure and are well separated, to avoid grain growth (Fig. 3). However, titanium atom has a relatively low electronegativity and can react rapidly in a nucleophilic reaction medium in which lignin, a polycyclic and three-dimensional mesh organic macromolecule with several electronegative OH groups, should have strong affinity for the positively charged metal ions; lignin with phenolic hydroxyl, alcoholic hydroxyl, and carboxyl groups can chemically react with other polymers to form hybrid composites. Lignin obtainable

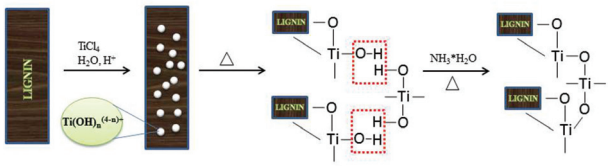

Fig. 3 Formation mechanism of mesoporous TiO_2 with lignin as a template.

from the black liquor waste of the paper-making process has great potential for the fabrication of TiO_2 particles filled with uniformly distributed nano-pores.[39,41]

3.2 TiO_2/STARBON®

Native polysaccharides are essentially non-porous and, therefore, their use is rather limited in applications where diffusion and surface interactions are required for optimum performance. Clark *et al.* pioneered a simple methodology to obtain highly expanded mesoporous polysaccharide materials (*e.g.* starch) from low surface area native starting materials.[42,43] Their synthesis entails three main steps: (1) formation of a gel by heating starch in water; (2) exchange of water with a lower surface tension solvent (*e.g.*, ethanol) at low temperature (≈5 °C); and (3) carbonization of the ensuing porous gels as-such or after drying to achieve the final mesoporous carbons (Fig. 4);[42,43] additional details are available on these synthetic methodologies[43–46] including TiO_2 supported on STARBON-800® as shown in Fig. 5.[48] Starbon® materials, derived from the controlled carbonization of different polysaccharides, exhibit chemical and surface properties that are intermediate between polysaccharides and carbons depending on the degree of carbonization;[42,43] their synthesis avoids the use of templates and can be performed at a temperature of choice (*e.g.*, 200–1000 °C). Another important feature is that these materials exhibit outstanding mesoporous textural properties, with pore volumes and sizes analogous to materials prepared *via* the traditional hard templating routes. The hydrophilic to hydrophobic nature of the carbonaceous product could be controlled by the degree of carbonization. Additionally, the flexible carbonization temperatures provide the possibility of tuneable surface chemistries, not accessible through hard templating (which generally needs higher temperatures, >700 °C) or soft templating processes based on polymeric organic templates (which limit the available post-processing surface functionalities). This simple and gentle process can produce a whole range of mesoporous carbon-based

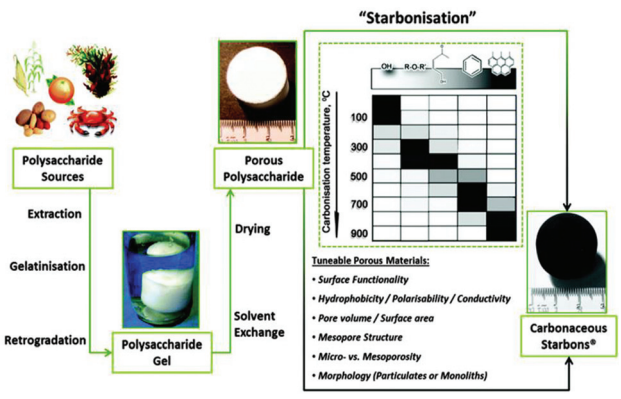

Fig. 4 A general overview of preparation of Starbons®, involving sourcing of the polysaccharide, followed by the preparation of an aqueous gel, its controlled drying and subsequent conversion to carbonaceous Starbons®. Reproduced with permission from ref. 47.

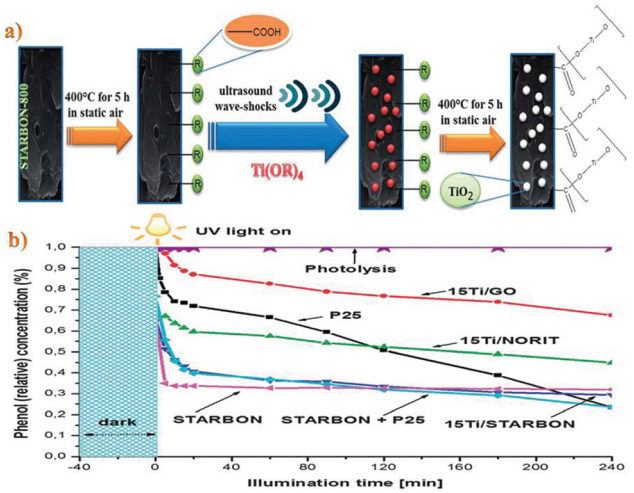

Fig. 5 (a) Schematic illustration of the plausible mechanism of the formation of TiO_2/STARBON hybrid material using ultrasound-assisted wet impregnation. (b) Photocatalyst activities in aqueous phase degradation of phenol (reaction conditions: 150 mL of mother solution, 150 mg of photocatalyst, C_{phenol} = 50 ppm, temperature 30 °C, reaction pressure 1 bar). Reproduced with permission from ref. 48.

materials, including amorphous carbon, that can serve as excellent catalysts or catalyst supports.[43–46] Interestingly, carboxylic groups can be formed on the surface after initial thermal treatment at 400 °C under an oxygen-deficient atmosphere (Fig. 5a). Then, each carboxyl group acts as an individual nucleation site for TiO_2 formation which is facilitated by hydrolysis and condensation reactions promoted *via* sonication. Finally, the hybrid material (TiO_2/STARBON®) is consolidated after thermal treatment at 400 °C in static air. These conditions preserve a pure and highly crystalline anatase phase (*ca.* 30 nm) leading to a reduction in the electron–hole recombination rate at the Starbon surface. TiO_2 is strongly anchored to the STARBON-800® structure as no leaching is observed even after 240 min of photocatalytic degradation of phenol (Fig. 5b); STARBON-800® enhances the photoelectron conversion of TiO_2 when compared to Norit and graphene oxide supports by reducing the recombination of photo-generated electron–hole pairs.[48] Coating TiO_2 photocatalyst on the surface of Starbon serves a dual purpose, *i.e.* it works as a support for nanosized TiO_2 which helps bring pollutants and intermediates around the TiO_2. Second, the TiO_2 can effectively destroy the adsorbed pollutants thus regenerating the Starbon *in situ* (only 3% of the initial concentration of phenol still stayed on Starbon surface after 240 minutes of reaction in comparison with 8.7% for STARBON+P25).

3.3 TiO_2/cellulose

Novel TiO_2/cellulose composites with interfacial silica and siloxane barriers have been prepared.[49] Vegetable cellulosic fibers have been surface modified *via* the hydrolysis of tetraethoxysilane (TEOS), octyltrimethoxysilane (OTMS) or phenyltrimethoxysilane (PTMS), followed by the layer-by-layer

deposition of previously synthesized TiO_2 nanoparticles. Distinct properties were realised for the cellulosic nanocomposites determined by the nature of the interlayer; while hydrophilic TiO_2/SiO_2/cellulose composites were generated by hydrolysis of TEOS, the OTMS and PTMS treated fibres (TiO_2/OTMS/cellulose and TiO_2/PTMS/cellulose) showed hydrophobic characteristics. Subsequently, after sunlight irradiation, the nanocomposite containing untreated fibres acquired a yellow colour indicating the partial degradation of cellulose fibres. Conversely, all the surface modified TiO_2 cellulose nanocomposites remained colourless even after several weeks of exposure to sunlight. Therefore, TiO_2/cellulose nanocomposites, in view of their compatibility with polymer matrices (hydrophobic or hydrophilic) are considered as forerunners for several applications, including self-cleaning materials and air purification filters. Previous research[50] has shown that the visible light activated TiO_2/microcrystalline cellulose (MC) nanocatalyst was photocatalytically active in degrading nearly 90% of methylene blue (MB) in 4 h (1 : 4 Ti^{4+}/MC synthesis conditions). As soon as electron is trapped by the molecular oxygen present on the TiO_2 surface, highly active radicals are generated which are responsible for the photo-bleaching of MB molecules; this obeyed first-order reaction kinetics with reaction constants of 5.02×10^{-3} min^{-1}. The TiO_2/MC nanocomposite benefits from the synergistic effect of the physical and/or chemical interactions between the organic and inorganic components and therefore could be utilized as a photocatalyst to degrade hazardous contaminants *via* the formation of films that have good mechanical and UV-shielding properties and in the synthesis of transition-metal carbide materials.[50] On similar lines, Zeng *et al.*[51] prepared TiO_2/cellulose composite films, which provided a cavity for the creation of TiO_2 nanoparticles, and hydroxyl groups for their immobilization. The prepared materials exhibited a good photocatalytic activity for the photodegradation of high concentration of phenol (67.2 mg L^{-1}) under weak UV light irradiation (0.56 mW cm^{-2}). Another elegant strategy for the preparation of TiO_2 nanomaterials has been described[52] that applies natural cellulose whiskers, obtainable by hydrolysis of native cellulose as templates. TiO_2/cellulose whisker nanoparticles exhibited quantum size effects and a lower band gap energy (2.02 eV) and displayed promising activity for the photodegradation of a methyl orange solution under weak UV light irradiation (4.3–41 mW cm^{-2}). They exhibited good stability against photocorrosion, implying that they could be used in the photodegradation of organic pollutants. It is worth noting that the regenerated cellulose films and fibers in the wet state possess a porous structure and the hydroxyl groups assist the creation of inorganic nanoparticles in the cellulose matrix.[53–56] Marques *et al.*[57] examined sheets prepared using a mixture of synthetic TiO_2/cellulose nanocomposite. The obtained composite exhibited a much higher opacity than those obtained by mechanical blending of the fibres with commercial TiO_2 pigment because of the highly homogeneous distribution of TiO_2 and higher specific surface area available for light scattering in sheets with the hybrid material. Such hybrids could be used as reinforcing fibers in a polymer matrix, particularly when light-barrier materials are sought. An interesting concept that involved the preparation of titanium dioxide nanocrystals on cellulose fibers (CF) by *in situ* hydrolysis has been reported;[58] TiO_2/CF composite showed enhanced adsorption capacity, good regenerability and selectivity for lead (Pb^{2+}) removal. Moreover, the adsorption capacity of a filter bed comprising nanocomposite fibers increased 12-fold as compared to the pure cellulose fiber bed; abundant hydroxyl groups on the CF surface adsorb TiO^{2+} first as nucleation sites and then TiO_2 nuclei are formed *via* hydrolysis-condensation which subsequently grow into TiO_2 nanocrystals. Meanwhile, the hydroxyl groups of cellulose would preferentially adsorb onto a certain crystallographic plane of TiO_2 due to anisotropy in adsorption stability. The approach described herein for material preparation and application are likely to offer an alternative versatile and greener pathway for fabricating a low cost, high efficiency engineering application as potential nanosorbents for heavy metal removal from water.

3.4 TiO_2/chitosan

Chitosan (poly-β-(1→4)-2-amino-2-deoxy-D-glucose), obtained by *N*-deacetylation (usually over 75%) of chitin, is the next most abundant natural polysaccharide after cellulose (Fig. 6)[59] and comprises the exoskeleton of insects and crustaceans (seafood processing industries' waste products) and cell walls of fungi.[60,61] Chitosan contains a large number of amino ($-NH_2$) and hydroxyl (–OH) functional groups and possesses excellent adsorption ability for a wide variety of environmental pollutants such as heavy metals,[62] dyestuffs,[62] and pathogens[63] and can be easily functionalized.[64] Furthermore, chitosan exhibits antibacterial activity, film forming ability and a good drug delivery potential.[65] The amino groups of chitosan can be easily cationized which help adsorb anionic dyes strongly *via* electrostatic attraction in acidic media. However, chitosan is very sensitive to pH as it can either form a gel or dissolve depending on the pH values.[59–65] Additionally, chitosan has some disadvantages such as unsatisfactory mechanical properties, severe shrinkage, deformation after drying, solubility under acidic conditions, compressibility at high operating

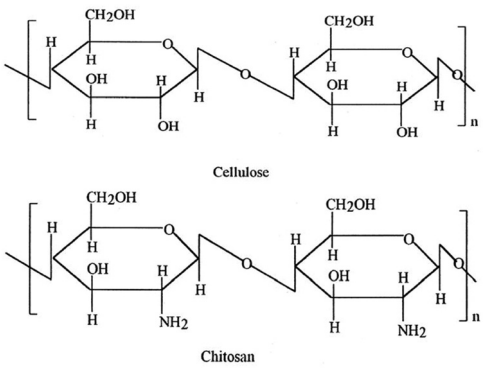

Fig. 6 Structures of cellulose and chitosan.

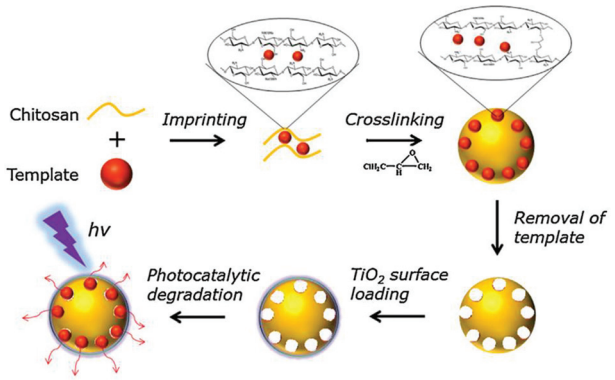

Fig. 7 Schematic illustration of the preparation process of the surface imprinted TiO_2/chitosan composite. Reproduced with permission from ref. 67.

pressure and can shield and block UV radiation with degradation of textiles and leather.[59,65,66] Previous research[67] has showed the efficacy of a novel methyl orange imprinted core–shell TiO_2/chitosan hybrid material (SICT) in selective photocatalytic degradation of methyl orange in dual-dye systems (Fig. 7). In this context, chitosan as a support for TiO_2 has following advantages: (a) easy recovery and multiple reuseability; (b) selectivity for target pollutants; (c) degradation and complete mineralization of organics; and (d) synergistic effect of the photocatalysis–adsorption processes of TiO_2/chitosan leading to lowering of the charge carrier recombination.[68] In addition, SICT could be reused directly without further desorption and regeneration for 10 cycles while retaining 60% of its photocatalytic efficiency. The reusability of SICT would be beneficial for simplification of the operating steps and the associated cost reduction would facilitate its practical application in wastewater treatment for environmental organic pollutants. Although chitosan has shown promise as a biosorbent, the chemical stability of chitosan is unsatisfactory because the abundant free amines, with a pK_a value of ~6.5, can be protonated culminating in hydro-solubility under acidic conditions.[67,68]

3.5 TiO_2/cellulose acetate

Cellulose acetate (CA) is biodegradable, nontoxic and biocompatible and can be prepared by simple esterification of cellulose, which is abundant in agricultural waste such as straw and biomass residues.[69–72] Cellulose acetate possess beneficial mechanical strength that facilitates its processing into films, membranes, and fibers from either melts or solutions. Further, due to paucity of hydrogen bonds and its lower crystallinity, its solubility in a wide range of organic solvents like acetone, dimethylformamide (DMF), dimethylsulfoxide (DMSO) *etc*. is enhanced.[73] The study of a flexible mesoporous TiO_2 microspheres/cellulose acetate (TCA) hybrid film (Fig. 8a),[74] showed that it can be easily recycled without a decrease in its activity for the degradation of methylene blue trihydrate solution (Fig. 8b). The TCA hybrid film displays stronger adsorption and photocatalytic degradation abilities

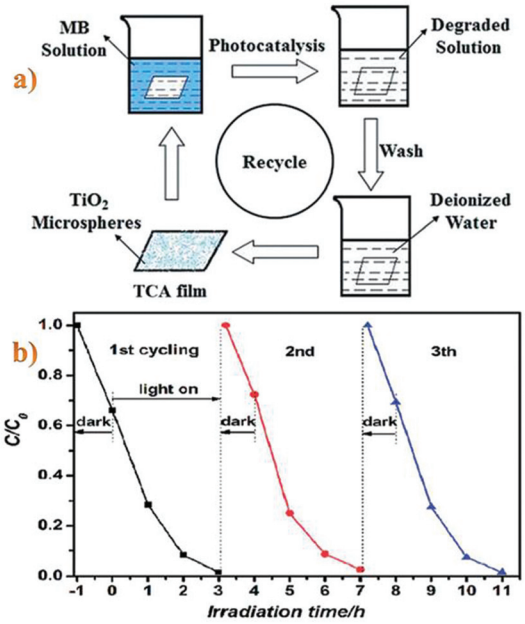

Fig. 8 (a) Schematic illustration of cellulose acetate (TCA) hybrid film recycling for use as a photocatalyst. (b) Photocatalytic activity of the sample TCA hybrid film on MB degradation with recycling (three times). Reproduced with permission from ref. 74.

for methylene blue when compared to a cellulose acetate film under the same conditions. The TCA hybrid film with its flexible, transparent and environmentally friendly properties, can be used as a self-cleaning material thus finding suitable application in the field of wastewater treatment without leaving any photocatalyst in the reaction system. A TiO_2/CA membrane prepared from DMF solution has a considerably better catalytic activity than the corresponding membrane obtained from acetone solution. By increasing the amount of TiO_2 in the composite, in the photocatalytic activity of the membrane was discerned until a certain value; increasing the TiO_2 content beyond that level led to lower catalytic activity.[74]

3.6 TiO_2/bacterial cellulose

Bacterial cellulose (BC), produced by acetic acid bacteria *Gluconobacter xylinum*, is obtainable in a pure form which requires no intensive processing to remove undesirable impurities and contaminants such as lignin, pectin and hemicellulose.[75,76] BC embodies several distinguished structural features and qualities such as good mechanical properties, biocompatibility, elevated tensile strength, a higher degree of polymerization (up to 8000), high crystallinity (of 70–80%), high water content (99%) and retention capability.[77,73–80] Another notable feature of BC is its high aspect ratio and abundant active functional hydroxyl groups, which make it suitable for combination with assorted nanostructures *via* its powerful interaction with surrounding species, such as inorganic and polymeric nanoparticles and nanowires.[81] The photocatalytic mesoporous TiO_2/BC hybrid nanofibers have been fabricated by surface hydrolysis with molecular precision;[82] uniform and

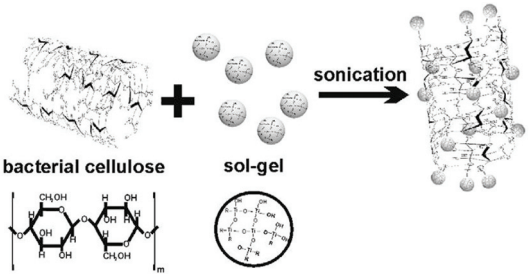

Fig. 9 Illustration of the synthesis of TiO_2/BC composites. Reproduced with permission from ref. 85.

well-defined nanofibers comprise large quantities of oriented TiO_2 nanoparticle arrays implanted on the BC nanofibers with diameters in the 4.3–8.5 nm range. A TiO_2/BC nanocomposite has been used as a photocatalyst for methyl orange degradation under UV irradiation, and it showed higher efficiency than the commercial photo-catalyst due to its high surface area (208.17 $m^2\ g^{-1}$). The BC template can be removed by calcination to afford mesoporous TiO_2 networks composed of interconnected anatase nanowires;[82,77–84] these networks exhibit considerably enhanced photocatalytic activity compared to the macroporous titania networks obtained through a similar sol–gel nanocasting procedure. The possible physical interactions between BC fibers and sol–gel solution in the TiO_2/BC hybrid fibers, facilitated by sonication (750 W), are shown in Fig. 9;[85] hydroxyl groups on the surface of the BC fibers provoke H-bonding interactions with the hydrophilic inorganic TiO_2 sol–gel network. TiO_2 nanoparticles respond to the applied voltage (−3, 0 and 3 V) of the electrostatic force microscopy (EFM) tip as the strong electrostatic dipole–dipole interactions are generated by hydrogen bonding connections between the hydroxyl groups in the cellulose and their counterparts in the inorganic oxide, thus eliciting a high electric dipole moment of TiO_2 nanoparticles in the TiO_2/BC hybrid fibers.

3.7 TiO_2/wood

Wood is a natural, sustainable and abundant biopolymeric material comprised of cellulose, hemicellulose, and lignin. Wood's natural hierarchical structure is composed of well-oriented microfibers and tracheids for water, ions, and oxygen transportation during metabolism; more importantly, multi-scale natural fibers from wood have unique optical properties applicable to different kinds of optoelectronics and photonic devices.[86,87] However, in view of its hygroscopic and organic nature, wood is sensitive to humidity variations and fire, which can lead to dimensional and thermal instability. Wood also features numerous hydroxyl groups that confer a hydrophilic nature on the cell wall which traps the polymeric Ti–OH inside the wood samples by interaction with wood hydroxyl.[86] The preparation of TiO_2/wood under mild ultrasonic conditions (*i.e.*, relatively low sonication intensity and low temperature) for a short period of time is presented in Fig. 10;[87] ultrasound provides a good distribution of TiO_2 throughout the wood matrix wherein these gels are deposited in the lumen by

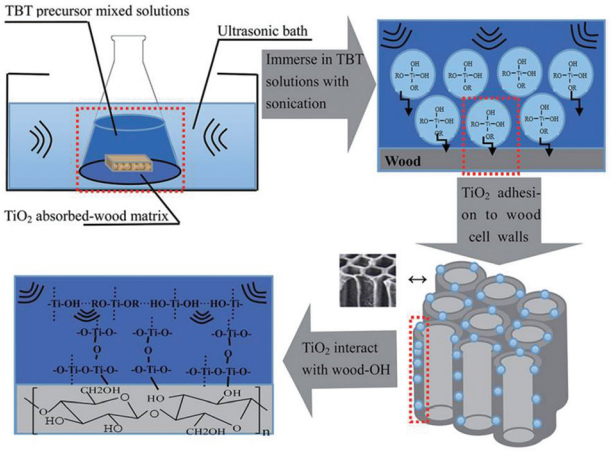

Fig. 10 Schematic of experimental set-up for preparing a TiO_2/wood matrix by the ultrasonic-assisted sol–gel method. Reproduced with permission from ref. 87.

adhesion to cell walls. Consequently, the cell wall components are obstructed from access to oxygen and complete combustion is delayed, thus enhancing the thermal stability of the wood. The modified wood possesses improved the thermal and mechanical properties and dimensional stability with increasing load of inorganic TiO_2 gels, as ultrasonic treatment facilitates chemical reactions between liquid and solid phases[88,89] thus helping the solution to be converted to polymeric TiO_2 inside the wood matrix. As each Ti is coordinated with four oxygen atoms, therefore the development of –Ti–O–Ti– chains results in three-dimensional polymeric skeletons with closed packing; wood materials with UV-resistant ability have been successfully fabricated by one-pot hydrothermal fabrication of rutile TiO_2 submicrospheres on the wood surface[90] as attested by ATR-FTIR spectra. On the other hand, vacuum and ultrasonic methods both enhance the dimensional stability of wood, by preventing the formation of cracks, retarding combustion of the wood matrix and diminishing biological attack.[87,91] A similar hydrothermal deposition of TiO_2 particles on spruce (Picea Abies) wood has been developed for the preparation of TiO_2/wood composites at 75 °C in a relatively short time (up to 1 h)[91] that serves the dual purpose of wood impregnation and covering the porous inner and outer surface of wood with rutile particles as discerned by ATR-FTIR and Raman subtraction spectra; the presence of titania particles on the hydrothermally treated wood surface exhibited vibrational bands of TiO_2-wood interphase interactions confirming the anchoring sites of titanium ions on hemicellulose, cellulose and lignin.[92]

4. TiO_2/carbon materials derived from agricultural residues

Numerous carbon sources such as biochar, activated carbon, bamboo or wood charcoal, carbon waste and even fly ash from coal-fired power plants can be utilized, as shown below.

4.1 TiO_2/biochar

Biochar has been considered as a potential surrogate for activated carbon and is produced by thermal decomposition (*e.g.*, slow pyrolysis, fast pyrolysis, hydrothermal carbonization (HTC), flash carbonization, torrefaction and gasification)[93–95] of a wide range of carbon-rich biomass materials that includes woody materials, agricultural residues such as sugarcane bagasse,[96] livestock manure,[97] and remnants after moderate temperature (*e.g.*, 350–700 °C) pyrolysis and carbonification of biomass in a reactor with little or no available air.[98–102] Non-activated biochar, *i.e.*, biochar that has not undergone any physical, chemical or biological modifications to improve its sorptive properties, can also be used as a precursor material for the production of activated carbon (Fig. 11). An important advantage of biochar over more conventional activated carbon is the presence of abundant surface functional groups (*e.g.* C–O, C═O, COOH, and OH, among others). Additionally, these groups show interesting catalytic properties due to the presence of O-, N-, and S-type functional groups, which serve as a platform for the synthesis of various functionalized carbon materials;[103–105] products, yields and characteristics of carbons derived from varied thermochemical conversion processes are illustrated in Fig. 11. The interaction of biochar with organic sorbates is dependent on the structural and chemical properties of the sorbates. The sorption of organic compounds by biochar, as illustrated in Fig. 12,[106] occurs by: (a) pore-filling mechanisms (contributed by the majority of the surface area of biochar); (b) diffusion and partitioning mechanisms (effects of electrostatic interactions on the diffusion and equilibrium partitioning); (c) surface hydrophobic and hydrophilic interactions; (d) aromatic– and cation–π interactions (*e.g.* strong, non-covalent π-electron donor–acceptor (EDA) interactions); (e) electrostatic interactions (sorption of ionic and ionizable organic compounds); and (f) hydrogen bonding (sorption of polar organic compounds) or by a simultaneous occurrence of all aforementioned mechanisms.[107,108] Biochar's uptake of organic solutes is a function of both surface and bulk properties of the carbonized (crystalline, graphene-like fractions) and non-carbonized fractions (non-crystalline, amorphous, organic carbon).[109,110] In order to promote heterogeneous photocatalytic reactions, Kim and Kan[111] developed surface-modified biochar (corn cob carbonized at 600 °C) and followed a simple sol–gel method to remove sulfamethoxazole (SMX) in water by photocatalytic oxidation using the biochar-supported TiO_2 photocatalyst under UV light irradiation (15 W UV-C, 254 nm). Surprisingly, the obtained composite showed a much higher adsorption of SMX than the commercial TiO_2 powder due to the hydrophobic interaction (carbon π–π interaction) between the biochar and SMX. It should be pointed out that photocatalytic oxidation of SMX using TiO_2/biochar under the selected catalyst loading and irradiation time (5 g L^{-1} of TiO_2/biochar, 6 h, pH 4) resulted in the highest removal and mineralization (91%, 81%, respectively) of SMX with negligible toxicity and accumulation of non-toxic products in water; three cycles of photocatalytic reactions using the same recycled catalyst resulted in the efficient removal of SMX (91%) confirming the high stability of the biochar-supported TiO_2 photocatalyst. An ecofriendly heterogeneous photocatalysis on biochar-based materials for methylene blue (MB) photodegradation under visible light (metal halide lamp) has been reported[112] wherein C-based materials induce enhancements in the photocatalytic environmental remediation of polluted water (phenol, halophenols, herbicides, dyes, azo-dyes, among others) and air (toluene, 2-propanol, among others); visible light-induced hydrogen photoproduction under solar irradiation is yet another outstanding example of photocatalytic energy storage by carbon-supported materials.

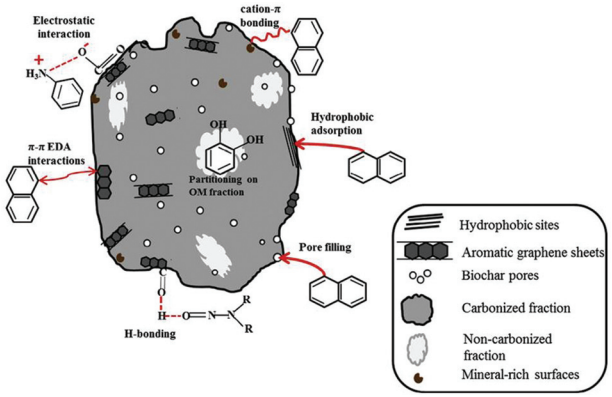

Fig. 12 Sorption mechanisms for the uptake of organic contaminants on biochar. Reproduced with permission from ref. 106.

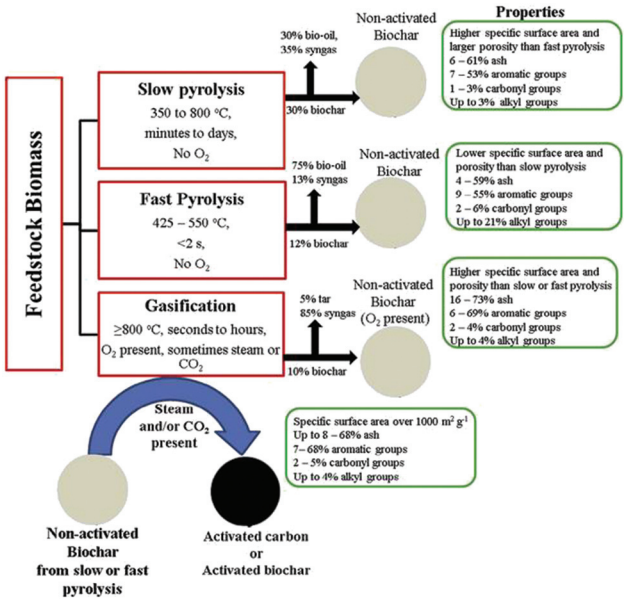

Fig. 11 Products, yields and characteristics of non-activated and physically activated biochars or carbons derived from biomass thermochemical conversion processes. Reproduced with permission from ref. 106.

4.2 TiO_2/activated carbon

Activated carbon (AC), also termed active carbon, activated charcoal, or activated coal, is a porous, amorphous solid carbon material derived mainly from carbonaceous or plant-based (lignocellulosic) materials such as coconut shell,[113–119] activated charcoal,[120] sawdust of *Tabebuia pentaphyla* wood,[121–124] pine sawdust,[125] beech sawdust,[126] peach stones,[127] almond shell activated carbon,[128,129] canola hull activated carbon,[130] cashew nut shell activated carbon,[131] water bamboo leaves,[132] and bituminous coal,[133] and can be used as a support for TiO_2. Furthermore, activated carbon adsorbs pollutants and then releases them onto the surface of TiO_2 thus delivering a higher concentration of pollutants around the TiO_2 than that available in the bulk solution culminating in an enhanced degradation rate of the pollutants; intermediates produced during degradation can also be adsorbed by AC which can then undergo further oxidation.[113] Nevertheless, the adsorption could generally enhance the photocatalytic rate but when the adsorption rate is much faster than the pollutant (*e.g.* methyl orange molecule) transfer rate, the photocatalytic kinetics are determined by the reaction rate on the TiO_2 surface.[134] Activated carbon has a well-developed pore structure with very large surface area and adsorption capacity and, consequently, possess a large number of active adsorption sites where organic molecules can be adsorbed before being transferred to the decomposition center of TiO_2;[113] oxidizing species ($^{\bullet}OH$) generated by the photocatalyst do not have to migrate very far from the active centers of the TiO_2 and degradation occurs on the catalyst surface. Using AC as a photocatalyst support conveys the pollutant molecules in close proximity to the titania active site (to come in contact with the hydroxyl radicals) for an efficient and effective photodegradation process (synergistic effect). AC can also function as a titania photosensitizer by injecting electrons into the conduction band of titania and triggering the photocatalytic formation of very reactive $^{\bullet}OH$ radicals which are responsible for the degradation of the dyes (*e.g.* Basic Red 18 and Basic Red 46).[130] In most cases, formate, acetate and oxalate have been detected as vital aliphatic carboxylic acid intermediates during the degradation of dyes. It is important to note that the initial formation of oxalate can increase with the illumination time, and then drop sharply. Furthermore, carboxylic acids can react directly with holes generating CO_2 according to the "photo-Kolbe" reaction:

$$R\text{–}COO^- + TiO_2(h_{VB}{}^+) \rightarrow TiO_2 + R^{\bullet} + CO_2.$$

In addition, photocatalytic mineralization of dyes implies the appearance of inorganic products, mainly anions, since heteroatoms are generally converted into anions at their highest oxidation state. On the other hand, TiO_2 has low selectivity because intermediate products of the photooxidation of aromatic molecules are commonly photomineralized.[135] In terms of the improvement of the photocatalytic properties of TiO_2, Matos *et al.*[122] investigated the changes of surface chemistry of the TiO_2/activated carbon during gasification and pyrolysis. It has been found that the interaction between TiO_2 and AC promotes higher concentrations of $O_2^{\bullet-}$ and $HO_2^{\bullet}$ radicals which induce remarkable changes in the selectivity of products. In addition, the synergistic effect could be attributed not only to a proper surface area but also to the presence of a low surface concentration of acidic oxygenated functionalities, particularly carboxylic groups. However, the surface carboxyl anions ($–COO^-$) are stabilized by transfer of electrons to the aromatic ring of graphene layers in activated carbon. Consequently, after dissociation in the aqueous phase, carboxylic acid (*e.g.* acetic acid) functional groups on the AC surface coordinate with the Ti^{4+} metallic center of TiO_2. Alternatively, this interaction could inhibit the recombination of photogenerated species in the semiconductor (e^-, h^+) thus forming a higher concentration of hydroxyl radical ($^{\bullet}OH$) and superoxide anion radical ($O_2^{\bullet-}$). The influence of the $O_2^{\bullet-}$ anion radical is very important because the higher the concentration of $O_2^{\bullet-}$, the higher is the production of $HO_2^{\bullet}$ radicals that enhance the photoactivity of TiO_2 in the photomineralization of 4-chlorophenol. It is worth noting that TiO_2 supported on AC will degrade total organic carbon (TOC)/phenol *via* a photocatalytic oxidation process.[128,129] Additionally, $^{\bullet}OH$ may attack aromatic ring sites in compounds resulting in the formation of ring-opened (Fig. 13) products yielding CO_2/H_2O and other degradation products;[136,137] breakdown of the benzene ring and its subsequent mineralization leading to CO_2 and H_2O could be envisaged by the decrease in TOC during the photocatalytic process.[138] Moreover, AC as a support for TiO_2 is effective in getting high rates of inactivate bacteria (*E. coli*) in the water phase.[117] Interestingly, adsorbent supports provide a higher concentration of bacteria around the loaded TiO_2 *via* adsorption; the rate of *E. coli* inactivation in the presence of TiO_2/AC catalysts is mostly determined by TiO_2 particles and fits well a pseudo-first order kinetic equation. Furthermore, bacteria are inactivated on the photocatalyst surfaces and then further decomposed; the high prevailing inactivation efficiency of the composite prevents the repair of cells. The TiO_2/AC composite has been used in conjunction with microwave (MW)-enhanced photodegradation of Rhodamine B (RhB) for the destruction of the conjugated structure, which was much faster than the photocatalytic degradation methods.[118] A distinctive feature, that the TiO_2 surface becomes more hydrophobic under MW irradiation,[125]

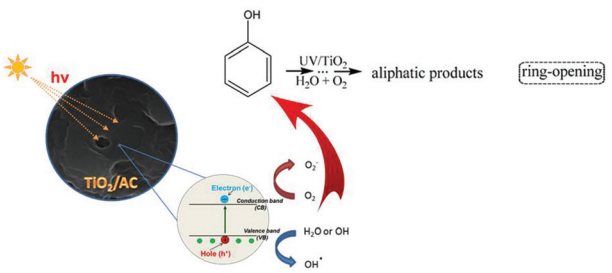

Fig. 13 Schematic illustration of the photocatalytic degradation of phenol by TiO_2/AC.

increases the probability of RhB contact with the TiO_2 surface. Additional defect sites on TiO_2 have been generated,[139] which can increase the transition probability of e^-/h^+ and decrease e^-/h^+ recombination on the TiO_2 surface. The strong interaction between TiO_2 and AC can be explained by the substrate transfer to titania where it is degraded photocatalytically.[140] In solution, the temperature of water and AC increases at different rates under MW irradiation due to in-core heating facilitated by MW energy which could generate locally higher temperature in some micro-surfaces of the AC particles compared to the water bulk.[141]

4.3 TiO_2/activated carbon with magnetic properties

Magnetic activated carbon derived from biomass waste[142,143] and soft magnetic ferrite activated carbon[144] have been commonly deployed as a support for TiO_2 possessing high surface areas and magnetic properties. Coconut shells or their lignocellulosic fractions, waste plant by-products that constitute a large fraction (~35%) of the total weight of coconut fruits, are good candidate precursors for magnetic activated carbon (MAC). Recently, magnetically separable TiO_2/MAC photocatalysts with high activity under solar illumination were synthesized and deployed for photocatalytic ozonation of metoprolol tartrate (MTP) in aqueous solution (50 mg L^{-1}) with high levels of photocatalytic mineralization (70–90%);[145] the MTP mineralization (*i.e.* conversion into CO_2) rate is highly depended on the anatase content of the catalyst. This photocatalyst was easily separable due to its magnetic properties, and its reusability and stability was successfully demonstrated in a series of 10 consecutive photocatalytic ozonation runs.

4.4 TiO_2/bamboo or wood charcoal

Bamboo is one of the most important non-timber forest products in the world and possesses high flexibility, high intensity, low weight, a fast growth rate and low purchasing costs. It has been extensively applied in a variety of daily applications such as indoor decoration, handicrafts, flooring construction, furniture, bamboo boats, and so forth.[146,147] However, bamboo is vulnerable to attack by fungi and termites on account of its inherent hygroscopicity and therefore, prone to lose its dimensional stability.[148] When exposed to an outdoor environment, unprotected bamboo shows bad decay resistance and is susceptible to attacks by fungi and insects, and degradation by moisture, air, acid rain, and sunlight thus shortening its service life and value.[149,150] The term charcoal generally refers to the carbonaceous residue of wood, cellulose, bamboo, coconut shells or various industrial wastes left behind after incomplete combustion of organic matter in the absence of oxygen;[151] usually it consists of carbon atoms, heteroatoms (mainly hydrogen and oxygen) and mineral matter (usually given as ash content). Wood charcoal is cheaper than AC because it doesn't need an activation process and has often been used for phenol adsorption.[152] The basic feature of wood charcoal is a highly aromatic matrix formed from layers of polycyclic aromatic rings bearing a content of organic carbon (53%) with a high C/N ratio; it can selectively adsorb hydrophobic rather than polar pollutants due to its non-polar nature.[153] A TiO_2/bamboo charcoal composite made by a dip-dry method is a porous adsorptive material which has a high specific surface area (359.8 m^2 g^{-1}), pore volume (0.317 cm^3 g^{-1}) and average pore diameter (3.526 nm).[154] Porous bamboo charcoal powder embedded in the matrix of TiO_2 particles has facilitated dye absorption and the generation of electrons during exposure to light.[155] Biotemplated synthesis of TiO_2/wood charcoal composites developed for the synergistic removal of bisphenol A (BPA) by adsorption and photocatalytic degradation is a recent example;[151] they displayed extraordinary adsorption ability for hydrophobic BPA and good photocatalytic activity (80% and 78%).

4.5 TiO_2/carbon waste and residues

Recently, Dávila-Jiménez *et al.*[156] prepared a series of TiO_2/carbon composite materials from carbonized avocado kernels and sols of TiO_2; their short preparation in fewer steps uses carbon with acidic groups that favors the interaction with TiO_2. The most efficient composites were obtained from carbons with the largest specific surface areas and a suitable micropore–mesopore ratio, favoring the immobilization of a larger amount of TiO_2 particles, regardless of the pHPZC of the carbon (pH where the carbon surface has neutral charge). Antonio-Cisneros *et al.*[157] immobilized TiO_2 on carbon emanating from residues of the plant *Manihot*, and this ensuing composite eliminated nearly 100% of the dye upon UV irradiation under optimal conditions; a similar investigation has been reported using carbon from *Manihot dulcis* waste,[158] and the TiO_2/carbon composite decomposed ~50% of carminic acid under various conditions. Interestingly, the adsorption is reversible, and the dye can be partially recovered by desorption, which can be advantageous in the case of artisanal carpeting effluents.

4.6 TiO_2/coal fly ash

Fly ash from coal, oil and biomass combustion are major contributors to the solid waste which is currently discarded in landfills or dumped at sea.[159] Coal fly ash (CFA) is a valuable and desirable additive to cement concrete because of its spherical shape and pozzolanic properties.[160,161] In other domains, coal fly ash is considered as a forerunner for several applications in adsorption,[162–164] material synthesis such as zeolites,[165–167] geopolymers,[168–170] ceramics,[171,172] and as a catalyst support.[173–175] Additionally, it has been shown that the prepared TiO_2/coal fly ash possesses potential advantages over the starting materials[176] such as: (a) the microspherical CFA particles are easy to precipitate in water, so photocatalysts supported on CFA are easy to recycle from aqueous solution after the reaction; (b) CFA, consisting primarily of Al_2O_3 and SiO_2 as support, can inhibit recombination of electrons and holes effectively;[177,178] (c) a porous structure is formed by the 3D network with additional loading of TiO_2 photocatalyst in its structure;[179] (d) the cost of preparation and the sources of environment pollution can be reduced. However, it is difficult to control uniform distribution of TiO_2 on CFA,[180,181] which

seriously restricts the activity of the photocatalyst and substrate availability. TiO_2 immobilized on the surface of CFA, the TiO_2/CFA composite, separates without difficulty from the treated wastewater by precipitation under quiescent conditions.[179] Since CFA particles are easy to precipitate in water because of their larger size and heavier weight compared to TiO_2 particles, the separation and recovery of the catalyst from water is facilitated when TiO_2 is immobilized on CFA. Therefore, TiO_2/CFA may be a promising material for applications in the removal of organic pollutants from water in the future.

4.7 TiO_2/biomaterials for degradation of organic pollutants

A biomaterial, derived from an organism, should have the inherent advantage to identify the majority of organic dye molecules effectively due to the high biocompatibility and structural complementarity of biomaterials towards organic pollutants. Biomaterials or biomimetic materials can identify dye molecules and selectively adsorb them as exemplified by eggshell on the surface of TiO_2-loaded composites.[182] Various studies have shown that TiO_2 loaded composites (*e.g.* TiO_2/skeleton,[182] TiO_2/DENs,[182] TiO_2/eggshell,[183] TiO_2/clamshell[183] and TiO_2/fish scale composites[184]) exhibited very high photocatalytic activity due to the synergistic effect of biomaterial association and the TiO_2 photocatalyst. Basically, nature-based biomaterials like fish scales are frequently used as adsorbents in biosorption processes due to their high binding capacities.[185] The uptake abilities of scales from different fish species should be similar because most fish scales contain significant portions of organic protein (collagen), and the structure of collagen contains alluring functional groups, such as phosphate, carboxyl, amine and amide, that are implicated in the biosorption process.[186]

5. Future prospects

This critical review summarizes most of the recent efforts on the syntheses and applications of TiO_2/carbon materials derived from renewable resources that, until a few years ago, were used as unique hybrid heterostructured photocatalysts for environmental remediation. TiO_2/carbon functional materials, with well-designed physical and chemical properties, will not only bring many favourable features to advanced oxidation processes but will provide a model system for investigating and understanding the dependence of photocatalytic performance on materials composition and structure at various scales, including fundamental studies on reaction mechanism and kinetics. Such an attained knowledge base, in turn, will greatly stimulate the better design of highly efficient hybrid photocatalysts. There are optimistic future expectations for the TiO_2/carbon materials derived from renewable resources in the field of photocatalysis and related fields of science. However, there are still a number of aspects that need to be addressed related to the rational and optimal design of materials; understanding of interphase interactions, especially under solar light conditions; novel energy-efficient processes; feedstock and production costs; issues related to carbon leaching from hybrid photocatalysts; and environmental impact concerns, to name a few. Despite much progress in photocatalysis, research on optimizing the properties of these photocatalysts is still in its infancy, as considerable challenges exist in terms of improving accurate structure–property relationships which need to be attended. Parallel to these advances, other allied applications for a greener and sustainable future are expected, namely in photodetectors, hybrid organic–inorganic solar cells, self-cleaning materials, air purification filters, photocorrosion-resistant materials, energy storage, CO_2 reduction, selective organic transformations and water splitting for hydrogen generation. Developments in these associated fields may unveil their enhanced understanding thus harnessing the power of these fascinating nanostructured materials.

Disclaimer

The views expressed in this article are those of the authors and do not necessarily represent the views or policies of the US Environmental Protection Agency. Any mention of trade names or commercial products does not constitute an endorsement or recommendation for use.

Acknowledgements

Prof. Dr Juan C. Colmenares gratefully acknowledges support from COST Action FP1306 for networking and possibilities for meetings and future students exchange. Paweł Lisowski would like also to thank the National Science Centre (NCN) in Poland for the research project 2015/17/N/ST5/03330.

References

1 D. S. Su, S. Perathoner and G. Centi, *Chem. Rev.*, 2013, **113**, 5782–5816.
2 Y. H. Ng, S. Ikeda, M. Matsumura and A. Amal, *Energy Environ. Sci.*, 2012, **5**, 9307–9318.
3 B. H. Nguyen, V. H. Nguyen and D. L. Vu, *Adv. Nat. Sci.: Nanosci. Nanotechnol.*, 2015, **6**, 1–13.
4 K. R. Reddy, M. Hassan and V. G. Gomes, *Appl. Catal., A*, 2015, **489**, 1–16.
5 G. Liu, L. Wang, H. G. Yang, H.-M. Cheng and G. Q. Lu, *J. Mater. Chem.*, 2010, **20**, 831–843.
6 Y. Qu and X. Duan, *Chem. Soc. Rev.*, 2013, **42**, 2568–2580.
7 M. Pelaez, N. T. Nolan, S. C. Pillai, M. K. Seery, P. Falaras, A. G. Kontos, P. S. M. Dunlop, J. W. J. Hamilton, J. A. Byrne, K. O'Shea, M. H. Entezari and D. D. Dionysiou, *Appl. Catal., B*, 2012, **125**, 331–349.
8 M. D. Hernandez-Alonso, F. Fresno, S. Suarez and J. M. Coronado, *Energy Environ. Sci.*, 2009, **2**, 1231–1257.
9 H. Wang, L. Zhang, Z. Chen, J. Hu, S. Li, Z. Wang, J. Liu and X. Wang, *Chem. Soc. Rev.*, 2014, **43**, 5234–5244.

10 J. Virkutyte and R. S. Varma, *RSC Adv.*, 2012, **2**, 2399–2407.
11 J. Virkutyte and R. S. Varma, *RSC Adv.*, 2012, **2**, 1533–1539.
12 J. Virkutyte, B. Baruwati and R. S. Varma, *Nanoscale*, 2010, **2**, 1109–1111.
13 J. Virkutyte and R. S. Varma, *New J. Chem.*, 2010, **34**, 1094–1096.
14 M. Pelaez, B. Baruwati, R. S. Varma, R. Luque and D. D. Dionysiou, *Chem. Commun.*, 2013, **49**, 10118–10120.
15 G. Varshney, S. R. Kanel, D. Kempisty, V. Varshney, A. Agrawal, E. Sahle-Demessie, R. S. Varma and M. N. Nadagouda, *Coord. Chem. Rev.*, 2016, **306**, 43–64.
16 M. N. Chong, B. Jin, C. W. K. Chow and C. Saint, *Water Res.*, 2010, **44**, 2997–3027.
17 S. Malato, P. Fernández-Ibáñez, M. I. Maldonado, J. Blanco and W. Gernjak, *Catal. Today*, 2009, **147**, 1–59.
18 R. Leary and A. Westwood, *Carbon*, 2011, **49**, 741–772.
19 C. O. Ania, L. F. Velasco and T. Valdes-Solis, *Novel Carbon Adsorbents*, Elsevier, 2012, pp. 521–547.
20 J. L. Faria and W. Wang, *Carbon Materials for Catalysis*, John Wiley & Sons, Inc., 2008, pp. 481–506.
21 Y. Zhai, Y. Dou, D. Zhao, P. F. Fulvio, R. T. Mayes and S. Dai, *Adv. Mater.*, 2011, **23**, 4828–4850.
22 R. J. White, V. Budarin, R. Luque, J. H. Clark and D. J. Macquarrie, *Chem. Soc. Rev.*, 2009, **38**, 3401–3418.
23 Q. F. Xu, Y. Liu, F.-J. Lin, B. Mondal and A. M. Lyons, *ACS Appl. Mater. Interfaces*, 2013, **5**, 8915–8924.
24 L. Su and Y. X. Gan, *Composites, Part B*, 2012, **43**, 170–182.
25 X. Wang, X. Xue, X. Liu, X. Xing, Q. Li and J. Yang, *Mater. Chem. Phys.*, 2015, **153**, 117–126.
26 S. Singh, H. Mahalingam and P. K. Singh, *Appl. Catal., A*, 2013, **462–463**, 178–195.
27 Y. Xia and R. C. Larock, *Green Chem.*, 2010, **12**, 1893–1909.
28 S. Dutta, A. Bhaumik and K. C.-W. Wu, *Energy Environ. Sci.*, 2014, **7**, 3574–3592.
29 M.-M. Titirici, R. J. White, C. Falco and M. Sevilla, *Energy Environ. Sci.*, 2012, **5**, 6796–6822.
30 I. Delidovich, K. Leonhard and R. Palkovits, *Energy Environ. Sci.*, 2014, **7**, 2803–2830.
31 S. Lacombe and T. Pigot, *Catal. Sci. Technol.*, 2016, **6**, 1571–1592.
32 H. Park, H.-I. Kim, G.-h. Moon and W. Choi, *Energy Environ. Sci.*, 2016, **9**, 411–433.
33 J. Shi, *Chem. Rev.*, 2013, **113**, 2139–2181.
34 A. Brandt, J. Gräsvik, J. P. Halletta and T. Welton, *Green Chem.*, 2013, **15**, 550–583.
35 C. Li, X. Zhao, A. Wang, G. W. Huber and T. Zhang, *Chem. Rev.*, 2015, **115**, 11559–11624.
36 G. W. Huber, S. Iborra and A. Corma, *Chem. Rev.*, 2006, **106**, 4044–4098.
37 A. Corma, S. Iborra and A. Velty, *Chem. Rev.*, 2007, **107**, 2411–2502.
38 D. M. Alonso, J. Q. Bond and J. A. Dumesic, *Green Chem.*, 2010, **12**, 1493–1513.
39 H. Kobayashi and A. Fukuoka, *Green Chem.*, 2013, **15**, 1740–1763.
40 R. F. Perez and M. A. Fraga, *Green Chem.*, 2014, **16**, 3942–3950.
41 X. Chen, D.-H. Kuo, D. Lu, Y. Hou and Y.-R. Kuo, *Microporous Mesoporous Mater.*, 2016, **223**, 145–151.
42 V. Budarin, J. H. Clark, J. J. E. Hardy, R. Luque, K. Milkowski, S. J. Tavener and A. J. Wilson, *Angew. Chem., Int. Ed.*, 2006, **45**, 3782–3786.
43 V. Budarin, J. H. Clark, J. J. E. Hardy, R. Luque, K. Milkowski, S. J. Tavener and A. J. Wilson, *Angew. Chem.*, 2006, **118**, 3866–3870.
44 V. L. Budarin, J. H. Clark, R. Luque and D. J. Macquarrie, *Chem. Commun.*, 2007, 634–636.
45 J. H. Clark, V. Budarin, T. Dugmore, R. Luque, D. J. Macquarrie and V. Strelko, *Catal. Commun.*, 2008, **9**, 1709–1714.
46 R. Luque, C. S. K. Lin, C. Du, D. J. Macquarrie, A. Koutinas, R. Wang, C. Webb and J. H. Clark, *Green Chem.*, 2009, **11**, 193–200.
47 M.-M. Titirici, R. J. White, N. Brun, V. L. Budarin, D. S. Su, F. del Monte, J. H. Clark and M. J. MacLachlan, *Chem. Soc. Rev.*, 2015, **44**, 250–290.
48 J. C. Colmenares, P. Lisowski and D. Łomot, *RSC Adv.*, 2013, **3**, 20186–20192.
49 G. Goncalves, P. A. A. P. Marques, R. J. B. Pinto, T. Trindade and C. P. Neto, *Compos. Sci. Technol.*, 2009, **69**, 1051–1056.
50 J. Virkutyte, V. Jegatheesan and R. S. Varma, *Bioresour. Technol.*, 2012, **113**, 288–293.
51 J. Zeng, S. Liu, J. Cai and L. Zhang, *J. Phys. Chem. C*, 2010, **114**, 7806–7811.
52 S. Liu, D. Tao, H. Bai and X. Liu, *J. Appl. Polym. Sci.*, 2012, **126**, 1–9.
53 J. Zeng, R. Li, S. Liu and L. Zhang, *ACS Appl. Mater. Interfaces*, 2011, **3**, 2074–2079.
54 H. Rollins, F. Lin, J. Johnson, J. Ma, J. Liu, M. Tu, D. DesMarteau and Y. Sun, *Langmuir*, 2000, **16**, 8031–8036.
55 S. Liu, L. Zhang, J. Zhou and R. Wu, *J. Phys. Chem. C*, 2008, **112**, 4538–4544.
56 D. Ke, S. Liu, K. Dai, J. Zhou, L. Zhang and T. Peng, *J. Phys. Chem. C*, 2009, **113**, 16021–16026.
57 P. A. A. P. Marques, T. Trindade and C. P. Neto, *Compos. Sci. Technol.*, 2006, **66**, 1038–1044.
58 Y. Li, L. Cao, L. Li and C. Yang, *J. Hazard. Mater.*, 2015, **289**, 140–148.
59 M. N. V. R. Kumar, *React. Funct. Polym.*, 2000, **46**, 1–27.
60 H. Orelma, I. Filpponen, L. S. Johansson, J. Laine and O. J. Rojas, *Biomacromolecules*, 2011, **12**, 4311–4318.
61 C. D. Tran, S. Duri, A. Delneri and M. Franko, *J. Hazard. Mater.*, 2013, **252–253**, 355–366.
62 D. Reddy and S. M. Lee, *Adv. Colloid Interface Sci.*, 2013, **201–202**, 68–93.
63 S. Mallick, S. Sharma, M. Banerjee, S. S. Ghosh, A. Chattopadhyay and A. Paul, *ACS Appl. Mater. Interfaces*, 2012, **4**, 1313–1323.

64 V. K. Mourya and N. N. Inamdar, *React. Funct. Polym.*, 2008, **68**, 1013–1051.
65 L. Cordero-Arias, S. Cabanas-Polo, H. Gao, J. Gilabert, E. Sanchez, J. A. Roether, D. W. Schubert, S. Virtanene and A. R. Boccaccini, *RSC Adv.*, 2013, **3**, 11247–11254.
66 W. A. Lee, N. Pernodet, B. Li, C. H. Lin, E. Hatchwell and M. H. Rafailovich, *Chem. Commun.*, 2007, 4815–4817.
67 G. Xiao, H. Su and T. Tan, *J. Hazard. Mater.*, 2015, **283**, 888–896.
68 M. A. Nawi, A. H. Jawad, S. Sabar and W. S. W. Ngah, *Desalination*, 2011, **280**, 288–296.
69 J. Simon, H. P. Müllera, R. Kocha and V. Müller, *Polym. Degrad. Stab.*, 1998, **59**, 107–115.
70 N. Y. Abou-Zeid, A. I. Waly, N. G. Kandile, A. A. Rushdy, M. A. El-Sheikh and H. M. Ibrahim, *Carbohydr. Polym.*, 2011, **84**, 223–230.
71 D. Wang, G. Sun and L. W. Yu, *Carbohydr. Polym.*, 2011, **83**, 1095–1100.
72 B. E. Dale, *J. Chem. Technol. Biotechnol.*, 2003, **78**, 1093–1103.
73 A. Wittmar, D. Vorata and M. Ulbricht, *RSC Adv.*, 2015, **5**, 88070–88078.
74 X. Jin, J. Xu, X. Wang, Z. Xie, Z. Liu, B. Liang, D. Chen and G. Shen, *RSC Adv.*, 2014, **4**, 12640–12648.
75 D. Klemm, B. Heublein, H. P. Fink and A. Bohn, *Angew. Chem., Int. Ed.*, 2005, **44**, 3358–3393.
76 P. Ross, R. Mayer and M. Benziman, *Microbiol. Rev.*, 1991, **55**, 35–58.
77 D. Klemm, D. Schumann, U. Udhardt and S. Marsch, *Prog. Polym. Sci.*, 2001, **26**, 1561–1603.
78 A. Svensson, E. Nicklasson, T. Harrah, B. Panilaitis, D. L. Kaplan, M. Brittberg and P. Gatenholm, *Biomaterials*, 2005, **26**, 419–431.
79 W. Hu, S. Chen, J. Yang, Z. Li and H. Wang, *Carbohydr. Polym.*, 2014, **101**, 1043–1060.
80 H. S. Barud, T. Regiani, R. F. C. Marques, W. R. Lustri, Y. Messaddeq and S. J. L. Ribeiro, *J. Nanomater.*, 2011, 721631.
81 J. Huang and Y. Gu, *Curr. Opin. Colloid Interface Sci.*, 2011, **16**, 470–481.
82 D. P. Sun, J. Z. Yang and X. Wang, *Nanoscale*, 2010, **2**, 287–292.
83 D. Y. Zhang and L. M. Qi, *Chem. Commun.*, 2005, 2735–2737.
84 G. Yang, J. J. Xie, Y. X. Deng, Y. G. Bian and F. Hong, *Carbohydr. Polym.*, 2012, **87**, 2482–2487.
85 J. Gutierrez, A. Tercjak, I. Algar, A. Retegi and I. Mondragon, *J. Colloid Interface Sci.*, 2012, **377**, 88–93.
86 B. Unger, M. Bucker, S. Reinsch and T. Hubert, *Wood Sci. Technol.*, 2013, **47**, 83–104.
87 B. Wang, M. Feng and H. Zhan, *RSC Adv.*, 2014, **4**, 56355–56360.
88 B. T. T. Chu, G. Tobias, C. G. Salzmann, B. Ballesteros, N. Grobert, R. I. Todd and M. L. Green, *J. Mater. Chem.*, 2008, **18**, 5344–5349.
89 S. Mallakpour, M. Dinari and V. Behranvand, *RSC Adv.*, 2013, **3**, 23303–23308.
90 Q. Sun, Y. Lu, H. Zhang, H. Zhao, H. Yu, J. Xu, Y. Fu, D. Yang and Y. Liu, *Mater. Chem. Phys.*, 2012, **133**, 253–258.
91 P. Pori, A. Vilcnik, M. Petric, A. S. Skapin, M. Mihelcic, A. S. Vuk, U. Novak and B. Orel, *Appl. Surf. Sci.*, 2016, **372**, 125–138.
92 J. Li, H. Yu, Q. Sun, Y. Liu, Y. Cui and Y. Lu, *Appl. Surf. Sci.*, 2010, **256**, 5046–5050.
93 S.-H. Kong, S.-K. Loh, R. T. Bachmann, S. A. Rahim and J. Salimon, *Renewable Sustainable Energy Rev.*, 2014, **39**, 729–739.
94 S. Ren, H. Lei, L. Wang, Q. Bu, S. Chen and J. Wu, *RSC Adv.*, 2014, **4**, 10731–10737.
95 J. Han, X. Wang, J. Yue, S. Gao and G. Xu, *Fuel Process. Technol.*, 2014, **122**, 98–106.
96 Y. Yao, B. Gao, M. Inyang, A. R. Zimmerman, X. Cao, P. Pullammanappallil and L. Yang, *Bioresour. Technol.*, 2011, **102**, 6273–6278.
97 C. J. Atkinson, J. D. Fitzgerald and N. A. Hipps, *Plant Soil*, 2010, **337**, 1–18.
98 F. Lian, F. Huang, W. Chen, B. Xing and L. Zhu, *Environ. Pollut.*, 2011, **159**, 850–857.
99 Y. Yu and H. Wu, *Energy Fuels*, 2010, **24**, 5660–5668.
100 T. R. Brown, M. M. Wright and R. C. Brown, *Biofuels, Bioprod. Biorefin.*, 2011, **5**, 54–68.
101 D. A. Laird, R. C. Brown, J. E. Amonette and J. Lehmann, *Biofuels, Bioprod. Biorefin.*, 2009, **3**, 547–562.
102 O. Mašek, P. Brownsort, A. Cross and S. Sohi, *Fuel*, 2013, **103**, 151–155.
103 I. Velo-Gala, J. J. Lopez-Penalver, M. Sanchez-Polo and J. Rivera-Utrilla, *Appl. Catal., B*, 2013, **142–143**, 694–704.
104 J. Matos, *Top. Catal.*, 2015, 1–9.
105 R. A. Shawabkeh, M. Al-Harthi and S. M. Al-Ghamdi, *Energy Sources, Part A*, 2014, **36**, 93–103.
106 M. Inyang and E. Dickenson, *Chemosphere*, 2015, **134**, 232–240.
107 P. Zhang, H. Sun, L. Yu and T. Sun, *J. Hazard. Mater.*, 2013, **244–245**, 217–224.
108 C. Chen, W. Zhou and D. Lin, *Bioresour. Technol.*, 2015, **179**, 359–366.
109 B. Chen, D. Zhou and L. Zhu, *Environ. Sci. Technol.*, 2008, **42**, 5137–5143.
110 M. Keiluweit, P. S. Nico, M. G. Johnson and M. Kleber, *Environ. Sci. Technol.*, 2010, **44**, 1247–1253.
111 J. R. Kim and E. Kan, *J. Environ. Manage.*, 2016, **180**, 94–101.
112 J. Matos, *Top. Catal.*, 2016, **59**, 394–402.
113 X. Wang, Y. Liu, Z. Hu, Y. Chen, W. Liu and G. Zhao, *J. Hazard. Mater.*, 2009, **169**, 1061–1067.
114 M. Khraisheh, J. Kim, L. Campos, A. H. Al-Muhtaseb, G. M. Walker and M. AlGhouti, *Environ. Eng. Sci.*, 2013, **30**, 515–526.
115 M. Toyoda, Y. Nanbu, T. Kito, M. Himno and M. Inagaki, *Desalination*, 2003, **159**, 273–282.
116 Y. Li, S. Zhang, Q. Yu and W. Yin, *Appl. Surf. Sci.*, 2007, **253**, 9254–9258.

117 L. Youji, M. A. Mingyuan, W. Xiaohu and W. Xiaohua, *J. Environ. Sci.*, 2008, **20**, 1527–1533.
118 H. Zhong, Y. Shaogui, J. Yongming and S. Cheng, *J. Environ. Sci.*, 2009, **21**, 268–272.
119 C. Andriantsiferana, E. F. Mohamed and H. Delmas, *Environ. Technol.*, 2014, **35**, 355–363.
120 B. Ayoubi-Feiz, S. Aber, A. Khataee and E. Alipour, *Environ. Sci. Pollut. Res.*, 2014, **21**, 8555–8564.
121 J. Matos, J. M. Chovelon, T. Cordero and C. Ferronato, *Open Envrion. Eng. J.*, 2009, **2**, 21–29.
122 J. Matos, A. Garcia and P. S. Poon, *J. Mater. Sci.*, 2010, **45**, 4934–4944.
123 J. Matos, A. Garcia, T. Cordero, J.-M. Chovelon and C. Ferronato, *Catal. Lett.*, 2009, **130**, 568–574.
124 J. Matos, E. Garcia-Lopez, L. Palmisano, A. Garcia and G. Marci, *Appl. Catal., B*, 2010, **99**, 170–180.
125 M. Asiltürk and S. Şener, *Chem. Eng. J.*, 2012, **180**, 354–363.
126 A. E. Eliyas, L. Ljutzkanov, I. D. Stambolova, V. N. Blaskov, S. V. Vassilev, E. N. Razkazova-Velkova and D. R. Mehandjiev, *Cent. Eur. J. Chem.*, 2013, **11**, 464–470.
127 T. S. Jamil, M. Y. Ghaly, N. A. Fathy, T. A. Abd el-halim and L. Österlund, *Sep. Purif. Technol.*, 2012, **98**, 270–279.
128 A. Omri, S. D. Lambert, J. Geens, F. Bennour and M. Benzina, *J. Mater. Sci. Technol.*, 2014, **30**, 894–902.
129 A. Omri and M. Benzina, *Environ. Monit. Assess.*, 2014, **186**, 3875–3890.
130 N. M. Mahmoodi, M. Arami and J. Zhang, *J. Alloys Compd.*, 2011, **509**, 4754–4764.
131 S. Ragupathy, K. Raghu and P. Prabu, *Spectrochim. Acta, Part A*, 2015, **138**, 314–320.
132 D. Huang, Y. Miyamoto, T. Matsumoto, T. Tojo, T. Fan, J. Ding, Q. Guo and D. Zhang, *Sep. Purif. Technol.*, 2011, **78**, 9–15.
133 L. F. Velasco, J. B. Parra and C. O. Ania, *Appl. Surf. Sci.*, 2010, **256**, 5254–5258.
134 Y. J. Li, Z. J. Song, Z. P. Li, Y. Z. Ouyang and W. B. Yan, *Chem. J. Chin. Univ.*, 2007, **28**, 1710–1715.
135 J. M. Herrmann, C. Duchamp, M. Karkmaz, B. T. Hoai, H. Lachheb, E. Puzenat and C. Guillar, *J. Hazard. Mater.*, 2007, **146**, 624–629.
136 G. Xue, H. Liu, Q. Chen, C. Hills, M. Tyrer and F. Innocent, *J. Hazard. Mater.*, 2011, **186**, 765–772.
137 W. T. Tsai, M. K. Lee, T. Y. Su and Y. M. Chang, *J. Hazard. Mater.*, 2009, **168**, 269–275.
138 L. Lagunas-Allué, M. T. Martinez-Soria, J. S. Asensio, A. Salvador, C. Ferronato and J. M. Chovelon, *Appl. Catal., B*, 2010, **98**, 122–131.
139 S. Horikoshi, H. Hidaka and N. Serpone, *Environ. Sci. Technol.*, 2002, **36**, 1357–1366.
140 J. Matos, J. Laine and J. M. Herrmann, *Appl. Catal., B*, 1998, **18**, 281–291.
141 L. L. Bo, X. Quan, S. Chen, H. M. Zhao and Y. Z. Zhao, *Water Res.*, 2006, **40**, 3061–3068.
142 A. L. Cazetta, O. Pezoti, K. C. Bedin, T. L. Silva, A. P. Junior, T. Asefa and V. C. Almeida, *ACS Sustainable Chem. Eng.*, 2016, **4**, 1058–1068.
143 A. M. Balu, B. Baruwati, E. Serrano, J. Cot, J. Garcia-Martinez, R. S. Varma and R. Luque, *Green Chem.*, 2011, **13**, 2750–2758.
144 S. Wang and S. Zhou, *Appl. Surf. Sci.*, 2010, **256**, 6191–6198.
145 D. H. Quinonesa, A. Reya, P. M. Álvareza, F. J. Beltrána and P. K. Plucinski, *Appl. Catal., B*, 2014, **144**, 96–106.
146 S. H. Lin, L. Y. Hsu, C. S. Chou, J. W. Jhang and P. Wu, *J. Anal. Appl. Pyrolysis*, 2014, **107**, 9–16.
147 Y. Xiao, Q. Zhou and B. Shan, *J. Bridge. Eng.*, 2010, **15**, 533–541.
148 Y. Yu, Z. Jiang, G. Wang, G. Tian, H. Wang and Y. Song, *Wood Sci. Technol.*, 2012, **46**, 781–790.
149 K. Lu, *J. Wood Sci.*, 2006, **52**, 173–178.
150 S. Chang, T. Yeh and J. Wu, *Polym. Degrad. Stab.*, 2001, **74**, 551–557.
151 L. Luo, Y. Yang, M. Xiao, L. Bian, B. Yuan, Y. Liu, F. Jiang and X. Pan, *Chem. Eng. J.*, 2015, **262**, 1275–1283.
152 S. Mukherjee, S. Kumar, A. K. Misra and M. Fan, *Chem. Eng. J.*, 2007, **129**, 133–142.
153 M. B. Fernandes and P. Brooks, *Chemosphere*, 2003, **53**, 447–458.
154 C. Da-li, J. Shen-xue and Z. Qi-sheng, *For. Stud. China*, 2012, **14**, 240–245.
155 C.-S. Chou, C.-Y. Chen, S.-H. Lin, W.-H. Lu and P. Wue, *Adv. Powder Technol.*, 2015, **26**, 711–717.
156 M. M. Dávila-Jiménez, M. P. Elizalde-González, E. García-Díaz, V. Marín-Cevada and J. Zequineli-Pérez, *Appl. Catal., B*, 2015, **166–167**, 241–250.
157 C. M. Antonio-Cisneros, M. M. Dávila-Jiménez, M. P. Elizalde-González and E. García-Díaz, *Food Chem.*, 2015, **173**, 725–732.
158 C. M. Antonio-Cisneros, M. M. Dávila-Jiménez, M. P. Elizalde-González and E. García-Díaz, *Int. J. Mol. Sci.*, 2015, **16**, 1590–1612.
159 S. Muhammad, E. Saputra, H. Sun, J. de C. Izidoro, D. A. Fungaro, H. M. Ang, M. O. Tade and S. Wang, *RSC Adv.*, 2012, **2**, 5645–5650.
160 H. Cho, D. Oh and K. Kim, *J. Hazard. Mater.*, 2005, **127**, 187–195.
161 V. Heaquet, P. Ricou, I. Lecuyer and P. Le Cloirec, *Fuel*, 2001, **80**, 851–856.
162 S. B. Wang, Y. Boyjoo and A. Choueib, *Chemosphere*, 2005, **60**, 1401–1407.
163 S. B. Wang, Y. Boyjoo, A. Choueib and Z. H. Zhu, *Water Res.*, 2005, **39**, 129–138.
164 S. Wang and H. Wu, *J. Hazard. Mater.*, 2006, **136**, 482–501.
165 K. S. Hui and C. Y. H. Chao, *Microporous Mesoporous Mater.*, 2006, **88**, 145–151.
166 H. Tanaka, H. Eguchi, S. Fujimoto and R. Hino, *Fuel*, 2006, **85**, 1329–1334.
167 M. Gross-Lorgouilloux, P. Caullet, M. Soulard, J. Patarin, E. Moleiro and I. Saude, *Microporous Mesoporous Mater.*, 2010, **131**, 407–417.
168 Sindhunata, J. S. J. van Deventer, G. C. Lukey and H. Xu, *Ind. Eng. Chem. Res.*, 2006, **45**, 3559–3568.

169 J. G. S. van Jaarsveld, J. S. J. van Deventer and G. C. Lukey, *Mater. Lett.*, 2003, **57**, 1272–1280.
170 S. Wang, L. Li and Z. H. Zhu, *J. Hazard. Mater.*, 2007, **139**, 254–259.
171 E. Furlani, S. Bruckner, D. Minichelli and S. Maschio, *Ceram. Int.*, 2008, **34**, 2137–2142.
172 G. Qian, Y. Song, C. Zhang, Y. Xia, H. Zhang and P. Chui, *Waste Manage.*, 2006, **26**, 1462–1467.
173 S. B. Wang, G. Q. Lu and H. Y. Zhu, *Chem. Lett.*, 1999, **28**, 385–386.
174 S. Wang and G. Q. Lu, *Stud. Surf. Sci. Catal.*, 2007, **167**, 275–280.
175 S. B. Wang, *Environ. Sci. Technol.*, 2008, **42**, 7055–7063.
176 X. Cui, J. Shi, Z. Ye, Z. Zhang, B. Xu and S. Chen, *Int. J. Photoenergy*, 2014, 823078.
177 D. Zhao, C. Chen, Y. Wang, W. Ma, J. Zhao, T. Rajh and L. Zang, *Environ. Sci. Technol.*, 2008, **42**, 308–314.
178 W. Kim, T. Tachikawa, T. Majima and W. Choi, *J. Phys. Chem. C*, 2009, **113**, 10603–10609.
179 J.-W. Shi, S.-H. Chen, S.-M. Wang, P. Wu and G.-H. Xu, *J. Mol. Catal. A: Chem.*, 2009, **303**, 141–147.
180 B. Gao, P. S. Yap, T. M. Lim and T.-T. Lim, *Chem. Eng. J.*, 2011, **171**, 1098–1107.
181 Y.-T. Yu, *Powder Technol.*, 2004, **146**, 154–159.
182 J. Wang, C. Li, X. Luan, J. Li, B. Wang, L. Zhang, R. Xu and X. Zhang, *J. Mol. Catal. A: Chem.*, 2010, **320**, 62–67.
183 X. Chen, C. Li, J. Wang, J. Li, X. Luan, Y. Li, R. Xu and B. Wang, *Mater. Lett.*, 2010, **64**, 1437–1440.
184 L.-N. Ho, S.-A. Ong and Y. L. See, *Water, Air, Soil Pollut.*, 2012, **223**, 4437–4442.
185 W. T. Liu, Y. Zhang, G. Y. Li, Y. Q. Miao and X. H. Wu, *J. Fish Biol.*, 2008, **72**, 1055–1067.
186 S. Mustafiz, M. S. Rahaman, D. Kelly, M. Tango and M. R. Islam, *Energy Sources*, 2003, **25**, 905–916.

